Design of 256-ch neurochemical MEA probe

Kevin A. White
Department of Electrical and Computer Engineering
University of Central Florida
Orlando, FL, USA
kevin.white@ucf.edu

Brian N. Kim
Department of Electrical and Computer Engineering
University of Central Florida
Orlando, FL, USA
brian.kim@ucf.edu

2022 IEEE Biomedical Circuits and Systems Conference (BioCAS) | 978-1-6654-6917-3/22/$31.00 ©2022 IEEE | DOI: 10.1109/BioCAS54905.2022.9948577

Abstract— **Dopamine constitutes a significant portion of the catecholamine content in the brain and plays a distinct role in neuromodulation including directing motor control, motivation, reward, and cognitive function. For future neuroprobe technology, not only is simultaneous high-density neurochemical recording vital, temporal resolution plays a key part in the roles of the spatiotemporal distributions of catecholamines in the brain. In this work, we present a new probe design that contains a 256 microelectrode array with an integrated 256 transimpedance amplifier array capable of both amperometry and fast-scan cyclic voltammetry. Each amplifier in the array is capable of both modes of electrochemical detection with three gain settings for the voltammetry mode and occupies an area of 60 µm × 60 µm. The new probe enables a high-resolution spatiotemporal mapping of neurochemicals in the brain.**

Keywords—biosensors, electrochemical devices, fast-scan cyclic voltammetry, microelectrodes, neurochemical

I. INTRODUCTION

Dopamine constitutes approximately 80% of the catecholamine content in the brain and its heterogeneous spatial and temporal distribution in the brain plays distinct roles in neuromodulation including directing motor control, motivation, reward, and cognitive function [1]–[4]. Traditional carbon fiber electrode (CFE) electrochemical techniques can measure neurochemical signaling with sufficient temporal resolution, however, there are significant challenges toward increasing the density of electrodes, and therefore are limited toward spatial mapping. Alternatively, fMRI, fNIRS, and two-photon imaging are capable of high spatial resolution, but have low temporal resolution due to the slow kinetics of indicators and low frame acquisition rates [5], [6]. As we are only beginning to understand the complex spatiotemporal distribution of dopamine innervation in the brain, there is a developing need for updated neurotechnology that can map distributed neurochemicals both spatially and temporally.

For neurochemical detection, the electrochemical techniques amperometry and fast-scan cyclic voltammetry (FSCV) are used. Amperometry is an electrochemical technique that detects electroactive molecules by the oxidation phenomenon, where a molecule releases an electron to the electrode if its oxidation potential has been reached. Although this technique has excellent temporal resolution, it is commonly performed at a fixed potential and cannot differentiate distinct species of molecules. However, FSCV is performed with a cyclic potential and can differentiate species of molecules as the oxidation and reduction, the opposing counterpart to oxidation, electrochemical phenomena create unique signal signatures with the tradeoff of reduced temporal resolution. For future neuroprobe technology, not only is simultaneous high-density neurochemical recording vital, temporal resolution plays a key part in studying the dynamics of synaptic transmission and neurochemical species differentiation is vital to understanding the roles of the various catecholamines in the brain.

Recent technologies have been developed to provide the desired enhanced temporal and spatial resolution for electrochemical detection techniques using scalable CMOS technology. An array of 32 × 32 pixels capable of cyclic voltammetry (CV) has demonstrated its capability to detect DNA loop structures [7]. A device with 8192 electrodes and 64 readout channels, capable of amperometry and CV, has been demonstrated to successfully image electrochemical activity from a murine adrenal slice [8]. A device with 16 × 64 sensors capable of CV and amperometry has demonstrated the capacity for consistent results across the array for ferricyanide detection [9]. A device with 32 × 32 sensors that is capable of amperometry and CV has demonstrated its capability to record and characterize single secretion events from neuronal model cells, pheochromocytoma [10], [11]. Despite the advances achieved by these devices, they are not yet appropriate for *in vivo* probing of the deep-brain areas, such as the nucleus accumbens. It may be possible to interface each electrode in these high-density devices with external probes, but this introduces a complex wiring scheme to connect 100s of electrodes for high resolution mapping.

In this work, we present a new design that contains a 256 microelectrode array (MEA) with an integrated 256 amplifier array capable of amperometry and FSCV, which has been strategically developed to become a monolithic *in vivo* neuroprobe (Fig. 1). The presented amplifier has been modified from a previous design [12], [13] and now has a larger current dynamic range for FSCV. FSCV has voltage scan rates that can range from 200 – 1000 V/s, and this creates significant background current on the scale of 100s of nAs. The tradeoff for this larger background current is that similar concentrations of a

This work was supported by the National Science Foundation (NSF) under grant #2133225, and the United States Air Force Office of Scientific Research (AFOSR) under grant #FA9550-21-1-0117.

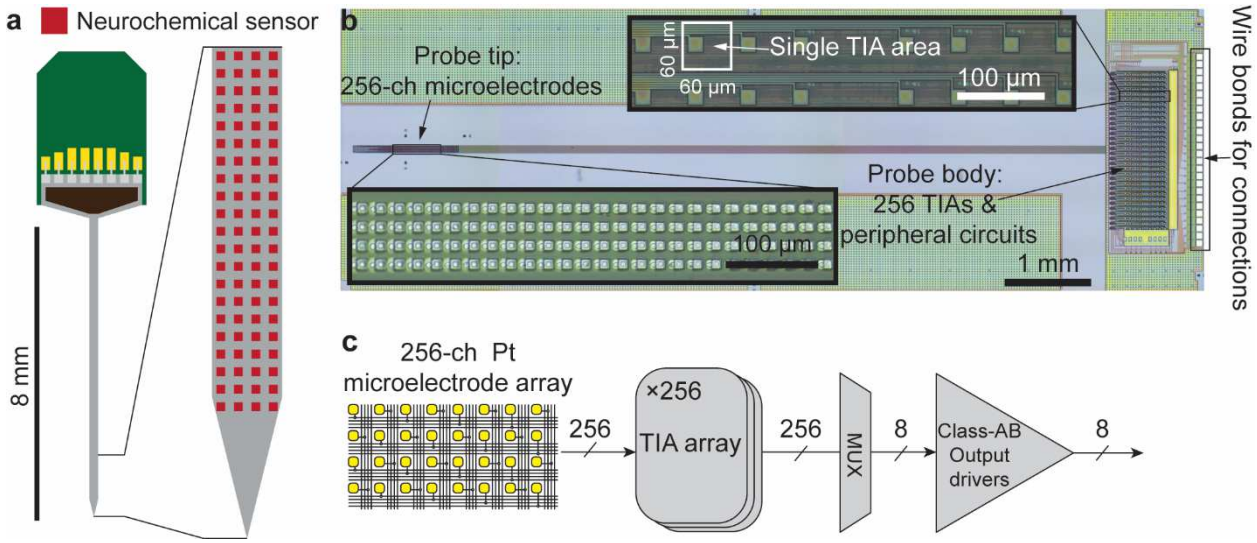

Figure 1. High-density neural probe design. (a) For monolithic *in vivo* neurochemical sensing, a shank contains neurochemical sensors at the tip and connects to integrated amplifiers at the body of the probe. (b) Microphotograph of the designed CMOS chip for *in vivo* neurochemical sensing. An array of 256 electrodes is located at one extreme of the silicon substrate and the integrated amplifier array and interfacing wirebonds are located at the other extreme of the substrate. The electrodes have a pitch of 20 µm and the amplifiers in the body occupy an area of 60 µm × 60 µm. (c) Each electrode is connected to a dedicated amplifier. The array of amplifiers is arranged in 8 columns and 32 rows, and each column of amplifiers is multiplexed, reducing the output of 256 neurochemical signals to 8 parallel data streams.

molecule generate a larger current as the scan rates increase. The previous design was an integrating transimpedance amplifier (TIA) design, wherein the output voltage of the amplifier is directly related to the magnitude of the input current that integrates onto a capacitor. The simplest way to increase the dynamic range would be to increase the integrating capacitor's capacitance, but this approach comes with nontrivial area requirements for FSCV level currents. In the approach presented, we use a current mirror that reduces the current from the electrode before it is integrated onto the integrating capacitor. In addition to the modified amplifier design, the strategic layout enables a shank shape to be etched out through post-CMOS processing, thus providing a high-density monolithic *in vivo* neuroprobe (Fig. 1).

II. High-Density Neural Probe

A high-density 256-ch neurochemical probe is developed that can operate parallel FSCV and amperometry from all electrodes for *in vivo* neurochemical imaging (Fig. 1). The presented probe is a monolithic probe design where the MEA is placed at of one extreme of the chip and the amplifier array is placed at the other extreme (Fig. 1b). This strategic layout of the electrode and amplifier arrays enables future post-CMOS processing to etch out a shank shape for *in vivo* brain implantation.

A. Design of Neurochemical Probe

The presented device was fabricated in a standard 0.35 µm CMOS process. The size of the chip is 10 mm × 3.4 mm, and the probe body is ~1.5 mm long, permitting a shank of ~8.5mm. The MEA is oriented in a 4 × 64 array to limit the width of the shank and each electrode is connected to a dedicated amplifier in the 8 × 32 amplifier array (Fig. 1c). Each column of amplifiers, containing 32 TIAs, is connected to its own dedicated multiplexer and output driver, thus reducing the 256 neurochemical sensors to 8 parallel outputs (Fig. 1c).

The designed TIA occupies an area of 60 µm × 60 µm, and is capable of both amperometry and the newly introduced FSCV mode of neurochemical sensing [12], [13]. When input CVon is low, the TIA is operating in amperometry mode as M8 cuts off the current path for transistors M9 – M15, which constitute the elements enabling FSCV mode (Fig. 2). In amperometry mode, the current from the electrode and M1 are integrated onto capacitor Cint, creating a current dependent voltage output that is read through the multiplexer that is enabled with transistors M5 – M7 where amplifiers throughout a column are selected based on the RowSelect input on transistor M6. At the end of the current integration cycle, the voltage at the bottom plate of Cint is readout and the reset transistor M4 restarts the integration cycle. For FSCV mode, the input CVon is high, thus transistor M3 prevents the reset of capacitor Cint and current is redirected to M9 – M15. Transistors M9 – M13 constitute a current mirror that attenuates the amplitude of current that is integrated onto the pMOS capacitor M15. The dimensions of M10 relative to M13 are 20:1 and M12 to M13 are 10:1. This enables three levels of current attenuation for FSCV mode, 30:1, 20:1, and 10:1 based on the settings for the inputs CVG0 and CVG1. The principal of current integration is similar to amperometry mode, wherein the current is integrated onto the gate connection of M15, the MOS capacitor for FSCV mode, creates a current dependent voltage output that is read through multiplexer transistors M16 – M18. At the end of the FSCV integration cycle, transistor M13 pulls the voltage of the pMOS cap's gate to a lower potential to remain in the linear region of capacitor operation for M15. The presented TIA design is not inherently capable of bipolar current measurement, which is vital for FSCV measurements. To enable bipolar measurement, transistor M1 sets a DC current point wherein current that is sourced or sunk from the electrode, due to either reduction or oxidation, can be detected as a change from the steady state setting of Ical [10].

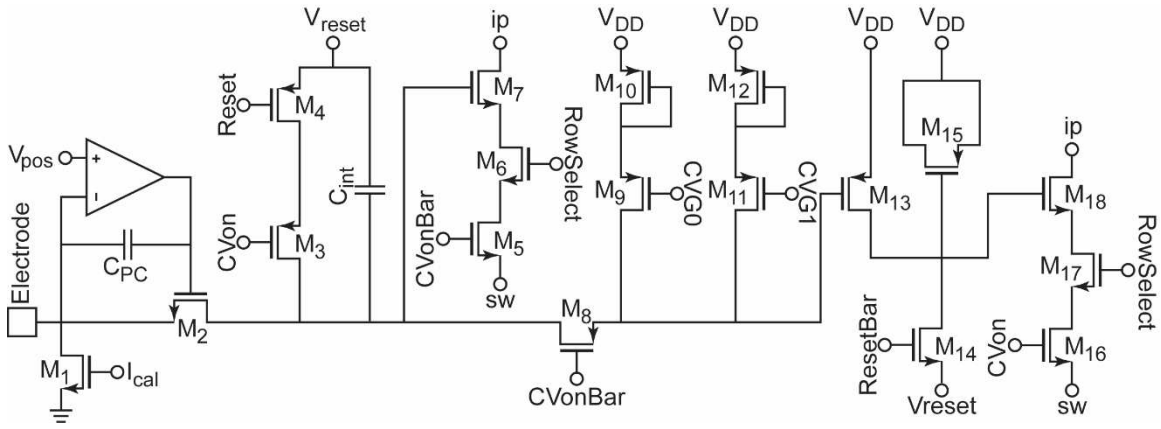

Figure 2. Neurochemical transimpedance amplifier design capable of amperometric and FSCV electrochemical measurements. The amplifier switches between amperometry mode and FSCV mode based on the input CVon. To enable bipolar current measurement, vital for cyclic voltammetry, transistor M1 can establish a DC current that is measured and the sourced or sunk current due to molecule oxidation or reduction, respectively, at the electrode is recorded as deviations from this DC setting.

B. *Neurochemical Amplifier Characteristics*

The performance characteristics for amperometry mode of the TIA have been explored in previous publications [12], [13]. The TIA exhibits ~0.4 pA_{RMS} at a 10 kHz sampling rate and has been shown to resolve single neurochemical secretion events from cells [12].

To characterize the new FSCV mode, the input current to output voltage gain throughout the amplifier's dynamic range is examined at a 40 kHz sampling rate. This output voltage vs input current curve is measured by applying known current through transistor M1 into the TIA and measuring the output voltage of the amplifier. A gain calibration curve for the change in output voltage vs input current was recorded for each gain setting and each setting exhibits excellent linearity (Fig. 3) with coefficients of determination, R^2, of 0.993 ± 0.004 (mean ± SD), 0.984 ± 0.006 (mean ± SD), and 0.993 ± 0.006 (mean ± SD) for settings 30:1, 20:1, and 10:1 respectively. The current-to-voltage gain is -1.50 ± 0.09 mV/nA (mean ± SD), -2.80 ± 0.15 mV/nA (mean ± SD), and -4.27 ± 0.27 mV/nA (mean ± SD) for settings 30:1, 20:1, and 10:1 respectively. Additionally, the noise of the TIA is ~2.42 nA_{RMS}, ~1.96 nA_{RMS}, and ~0.859 nA_{RMS} for settings 30:1, 20:1, and 10:1 respectively (Fig. 4).

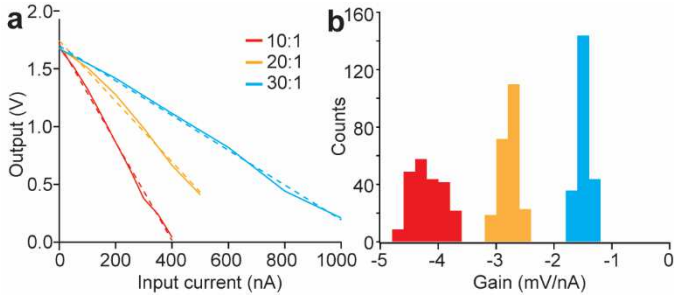

Figure 3. Cain calibration for FSCV mode. (a) Output voltage vs input current gain curves. Each gain setting exhibits excellent linearity throughout the dynamic range of the calibration curve (average R^2 is 0.993, 0.984, and 0.993 for settings 30:1, 20:1, and 10:1 respectively). (b) Histogram of the current-to-voltage gain of each TIA. The average gain values are -1.50 mV/nA, -2.80 mV/nA, and -4.27 mV/nA for settings 30:1, 20:1, and 10:1 respectively

C. *Post-CMOS Processing*

A platinum MEA is integrated onto the CMOS chip through photolithography processing as previously described [11]. A sacrificial layer of negative photoresist is first developed on the surface of the chip. Platinum is then deposited by a sputtering machine (200 nm) and the sacrificial layer of photoresist is removed, patterning the platinum electrodes. Silicon dioxide is then deposited on top of the platinum electrodes (300 nm) and etched to provide a passivation layer to the electrodes, which creates an effective electrode area of 5 µm in diameter. This electrode passivation enables single neurochemical secretion events resolution in amperometry mode by limiting the double-layer capacitance, which is directly influenced by the area of the electrode-electrolyte interface, and thus improves the noise performance of the TIAs [11].

III. FSCV Electrochemical Detection

The amperometric electrochemical detection capability of the TIA have been previously presented for single secretion events [11], [12]. Despite the excellent temporal resolution of amperometry, for *in vivo* differentiation of various neurochemical species, the newly introduced FSCV mode of electrochemical detection is necessary. From FSCV measurements, a unique signature reveals the composition of

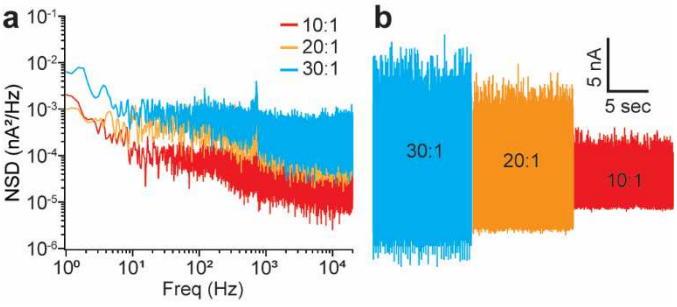

Figure 4. Noise performance of the TIA in FSCV mode at a 40 kHz sampling rate. (a) Noise spectral densities of the TIA at each gain setting (b) Noise of the TIA in the time domain. The noise of the amplifier is ~2.42 nA_{RMS}, ~1.96 nA_{RMS}, and ~0.859 nA_{RMS} for settings 30:1, 20:1, and 10:1 respectively

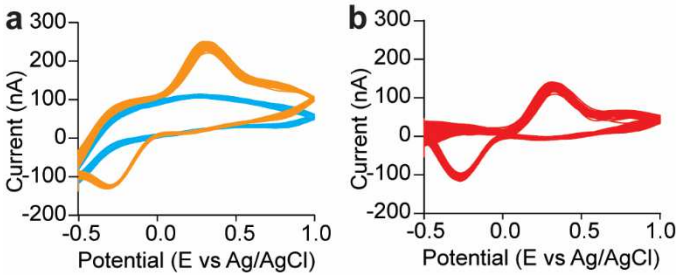

Figure 5. FSCV voltammograms from a Pt electrode. (a) Blue line is the voltammogram of an electrochemical recording in PBS solution. In the absence of electroactive molecules, this is a recording of the background noise from capacitive and resistive current. Orange line is the voltammogram of the Pt electrode in PBS solution containing 10 µM of ferrocyanide. The recorded current exhibits distinct current peaks at +0.31 V (oxidation) and -0.28 V (reduction). (b) Background-subtracted voltammogram obtained by subtracting the background current from the background plus electrochemical current from ferrocyanide. The background-subtracted voltammogram provides a clear indication of the oxidation (+0.31 V) and reduction (-0.28 V) peaks showing a response of ~+117 nA and ~-115nA respectively due to ferrocyanide.

electroactive molecules as different peaks in the captured current signal which are directly related to the oxidation and reduction potentials of a molecule as the electrode's potential sweeps through a voltage range.

The neurochemical probe is tested using ferrocyanide. For the FSCV electrochemical setup, an Ag|AgCl reference electrode is placed into the saline solution and is held at a potential of 0.7 V. The electrode potential, applied to node Vpos (Fig. 2), is swept from 0.2 to 1.7 V at a rate of 300 V/s and is repeated every 100 ms, providing a redox potential from -0.5 to 1.0 V.

A baseline FSCV recording is acquired by placing the electrodes into phosphate-buffered saline (PBS) solution. This resulting voltammogram reveals the capacitive and resistive current from the electrodes (Fig. 5a). Then the electrodes are placed into PBS solution that contains 10 µM of ferrocyanide. We can see a change in the recorded signal as a positive current peak (oxidation) at +0.31 V and a negative current peak (reduction) at -0.28 V (Fig. 5a). To better view only the oxidation and reduction current from the ferrocyanide molecules, we can subtract the background current from the recording with background and electrochemical currents. Background-subtracted voltammograms highlight the redox current of the molecule(s), ferrocyanide in this case, which are present at the electrode (Fig. 5b). At the oxidation (+0.31 V) and reduction (-0.28 V) potentials, the TIA measured electrochemical currents of ~+117 nA and ~-115nA respectively due to the ferrocyanide molecules present in the PBS.

IV. Conclusion

The presented high-density 256-ch neurochemical probe has been developed for *in vivo* neurochemical detection. The capability of the newly integrated FSCV mode has been characterized and demonstrated successful measurement of an electroactive molecule, ferrocyanide. Having both electrochemical detections methods provide excellent temporal resolution of fast neurochemical secretion events (amperometry) as well as sensitivity to low concentrations, ranging as low as 10s of nM, and differentiation of various electroactive neurochemicals in the brain (FSCV). By integrating these dual modes of detection with a large 256 electrode array, we will enable unprecedented levels of parallel neurochemical mapping with enhanced spatial, temporal, and concentration sensitivity.

V. Discussion

The future goal of this neurotechnology is to complete the post-CMOS processing procedure to etch out a shank from the CMOS chip for *in vivo* implantation. The currently explored approach to achieve an implantable probe is by exploring photolithographic processes combined with deep reactive ion etching [14]–[18]. Additionally, work must be done to characterize and catalog the different signal signatures of electroactive molecules to our system so that we can identify and quantify substances that are present in the brain.

References

[1] R. v. Bhimani, R. Yates, C. E. Bass, and J. Park, "Distinct limbic dopamine regulation across olfactory-tubercle subregions through integration of in vivo fast-scan cyclic voltammetry and optogenetics," *Journal of Neurochemistry*, vol. 161, no. 1, pp. 53–68, Apr. 2022, doi: 10.1111/JNC.15577.

[2] R. v. Bhimani, M. Vik, K. T. Wakabayashi, C. Szalkowski, C. E. Bass, and J. Park, "Distinct dose-dependent effects of methamphetamine on real-time dopamine transmission in the rat nucleus accumbens and behaviors," *Journal of Neurochemistry*, vol. 158, no. 4, pp. 865–879, Aug. 2021, doi: 10.1111/JNC.15470.

[3] A. L. Deal, J. Park, J. L. Weiner, and E. A. Budygin, "Stress Alters the Effect of Alcohol on Catecholamine Dynamics in the Basolateral Amygdala," *Frontiers in Behavioral Neuroscience*, vol. 15, p. 69, Apr. 2021, doi: 10.3389/FNBEH.2021.640651/BIBTEX.

[4] C. A. Owesson-White, J. F. Cheer, M. Beyene, R. M. Carelli, and R. M. Wightman, "Dynamic changes in accumbens dopamine correlate with learning during intracranial self-stimulation," *Proc Natl Acad Sci U S A*, vol. 105, no. 33, pp. 11957–11962, Aug. 2008, doi: 10.1073/PNAS.0803896105/SUPPL_FILE/0803896105SI.PDF.

[5] N. Li and A. Jasanoff, "Local and global consequences of reward-evoked striatal dopamine release," *Nature 2020 580:7802*, vol. 580, no. 7802, pp. 239–244, Apr. 2020, doi: 10.1038/s41586-020-2158-3.

[6] T. Lee, L. X. Cai, V. S. Lelyveld, A. Hai, and A. Jasanoff, "Molecular-level functional magnetic resonance imaging of dopaminergic signaling," *Science (1979)*, vol. 344, no. 6183, pp. 533–535, May 2014, doi: 10.1126/SCIENCE.1249380/SUPPL_FILE/LEE.SM.PDF.

[7] A. Manickam *et al.*, "A CMOS Electrochemical Biochip with 32 × 32 Three-Electrode Voltammetry Pixels," *IEEE Journal of Solid-State Circuits*, vol. 54, no. 11, pp. 2980–2990, Nov. 2019, doi: 10.1109/JSSC.2019.2941020.

[8] W. Tedjo *et al.*, "Electrochemical biosensor system using a CMOS microelectrode array provides high spatially and temporally resolved images," *Biosensors and Bioelectronics*, vol. 114, pp. 78–88, Aug. 2018, doi: 10.1016/J.BIOS.2018.04.009.

[9] M. Huang, C. I. Dorta-Quiñones, B. A. Minch, and M. Lindau, "On-Chip Cyclic Voltammetry Measurements Using a Compact 1024-Electrode CMOS IC," *Analytical Chemistry*, vol. 93, no. 22, pp. 8027–8034, Jun. 2021, doi: 10.1021/ACS.ANALCHEM.1C01132/ASSET/IMAGES/LARGE/AC1C01132_0012.JPEG.

[10] K. A. White, G. Mulberry, and B. N. Kim, "Parallel 1024-ch Cyclic Voltammetry on Monolithic CMOS Electrochemical Detector Array," *IEEE Sensors Journal*, vol. 20, no. 8, pp. 4395–4402, Apr. 2020, doi: 10.1109/JSEN.2019.2961809.

[11] K. A. White and B. N. Kim, "Quantifying neurotransmitter secretion at single-vesicle resolution using high-density complementary metal–oxide–semiconductor electrode array," *Nature Communications*, vol. 12, no. 1, pp. 1–8, Dec. 2021, doi: 10.1038/s41467-020-20267-0.

[12] K. A. White *et al.*, "Single-Cell Recording of Vesicle Release from Human Neuroblastoma Cells using 1024-ch Monolithic CMOS

Bioelectronics," *IEEE Transactions on Biomedical Circuits and Systems*, vol. 12, no. 6, pp. 1345–1355, 2018, doi: 10.1109/TBCAS.2018.2861220.

[13] G. Mulberry, K. A. White, and B. N. Kim, "Analysis of Simple Half-Shared Transimpedance Amplifier for Picoampere Biosensor Measurements," *IEEE Transactions on Biomedical Circuits and Systems*, vol. 13, no. 2, pp. 387–395, Apr. 2019, doi: 10.1109/TBCAS.2019.2897287.

[14] C. Zhao *et al.*, "Implantable aptamer-field-effect transistor neuroprobes for in vivo neurotransmitter monitoring," *Science Advances*, vol. 7, no. 48, p. 7422, Nov. 2021, doi: 10.1126/SCIADV.ABJ7422/SUPPL_FILE/SCIADV.ABJ7422_MOVIE_S1.ZIP.

[15] A. Novais *et al.*, "Hybrid Multisite Silicon Neural Probe with Integrated Flexible Connector for Interchangeable Packaging," *Sensors 2021, Vol. 21, Page 2605*, vol. 21, no. 8, p. 2605, Apr. 2021, doi: 10.3390/S21082605.

[16] L. Yang, K. Lee, J. Villagracia, and S. C. Masmanidis, "Open source silicon microprobes for high throughput neural recording," *Journal of Neural Engineering*, vol. 17, no. 1, p. 016036, Jan. 2020, doi: 10.1088/1741-2552/AB581A.

[17] E. Otte, V. Cziumplik, P. Ruther, and O. Paul, "Customized Thinning of Silicon-based Neural Probes Down to 2 μm," *Proceedings of the Annual International Conference of the IEEE Engineering in Medicine and Biology Society, EMBS*, vol. 2020-July, pp. 3388–3392, Jul. 2020, doi: 10.1109/EMBC44109.2020.9176523.

[18] C. M. Lopez, A. Andrei, S. Wang, R. van Hoof, S. Severi, and N. van Helleputte, "Design and fabrication of CMOS-based neural probes for large-scale electrophysiology," *Technical Digest - International Electron Devices Meeting, IEDM*, vol. 2019-December, Dec. 2019, doi: 10.1109/IEDM19573.2019.8993529.